Understanding relationship between melt/ freeze conditions derived from spaceborne scatterometer and field observations at Larsemann Hills, East Antarctica during austral summer 2015–16

Rajashree V. Bothale[1,*], S. Anoop[1], V. V. Rao[1], V. K. Dadhwal[2] and Y. V. N. Krishnamurthy[1]

[1]National Remote Sensing Centre (ISRO), Hyderabad 500 037, India
[2]Indian Institute of Space Science and Technology, Thiruvananthapuram 695 547, India

Snow fork and ground penetrating radar at 200 MHz were used for snow depth, wetness and density measurements towards understanding the relationship between melt/freeze conditions derived from spaceborne Advance Scatterometer (ASCAT) and Oceansat-2 Scatterometer (OSCAT), and field observations. The observations were acquired at Larsemann Hills, East Antarctica in austral summer of 2015–16 during the 35th Indian Scientific Expedition to Antarctica. The field observations of wetness correlated well with identified dry and percolation zones showcasing different behaviours of density and wetness. Ice firn was observed at 50–55 cm depth, even in dry zone. Melt onset and number of melt days based on ASCAT varied spatially and temporally over the years and correlated well with positive degree day (PDD) for automatic weather station data located at the Indian Antarctic station, Bharati. Backscatter measurements by OSCAT showed that winter backscatter reduced with accumulation for both dry and percolation zones, but increased in the later part of winter in the percolation zone. A positive but low correlation was observed between ASCAT backscatter to accumulation and the surface mass balance from regional atmospheric climate model (RACMO2.3). A high correlation of 0.78 was observed between reduction in backscatter due to liquid water content and PDD, which coincides with field observations of wetness. The observations serve as baseline to monitor melt conditions and stability of existing ice sheet.

Keywords: Ground penetrating radar, ice firn, snowfork, scatterometer, snowpack characteristics.

CLIMATOLOGICAL and hydrological applications require knowledge about spatio-temporal behaviour of melting snow and ice. Monitoring melt conditions can help predict the stability of existing ice sheets. Melting affects the run-off from shelves and sea ice. The melting and freezing cycles affect the snow metamorphism, which in turn changes the amount of solar radiation absorbed by the snow pack, thereby affecting the albedo and surface energy balance[1]. Complexity of snow structure and spatial variability makes the understanding of dielectric properties a difficult task. Dielectric properties control the interaction of electromagnetic waves with snow, affecting satellite remote sensing of wet and dry snow[2,3]. Satellite remote sensing provides crucial information over Antarctica, since very few ground observations have been made over the continent. Permittivity and density at six locations in Queen Maud land, Antarctica were measured, where it was observed that the measured, permittivity ε' was not well correlated with the snow density[4]. Dielectric measurements were carried out in Western Dronning Maud land, where less correlation between permittivity and density was observed[5]. Dielectric permittivity of the upper 1 m snow layer along the 2800 km long expedition route near Syowa and Wasa stations was measured; it was found to be a function of snow density[6]. Snow fork and other devices have been used in the Swiss Alps to observe point liquid water content in snowpack[7].

Snow melt and freeze conditions using *in situ* measurement have been reported by many researchers but owing to difficult terrain and inaccessibility, they have used satellite remote sensing to obtain spatial distribution of melt[8–11]. Investigation of wet snow is a challenging task as liquid water in the snow affects snowpack characteristics. Presence of ice layer and lenses also affect the overall characteristics of snowpack. Owing to difficulties of field measurements, there is a need to correlate the satellite-based observations with field observations so that analysis using satellite data in the future could be taken up in the absence of field data.

*For correspondence. (e-mail: rbothale@gmail.com)

Figure 1. Ground penetrating radar observations over ice sheet and snow fork observations inside the pit.

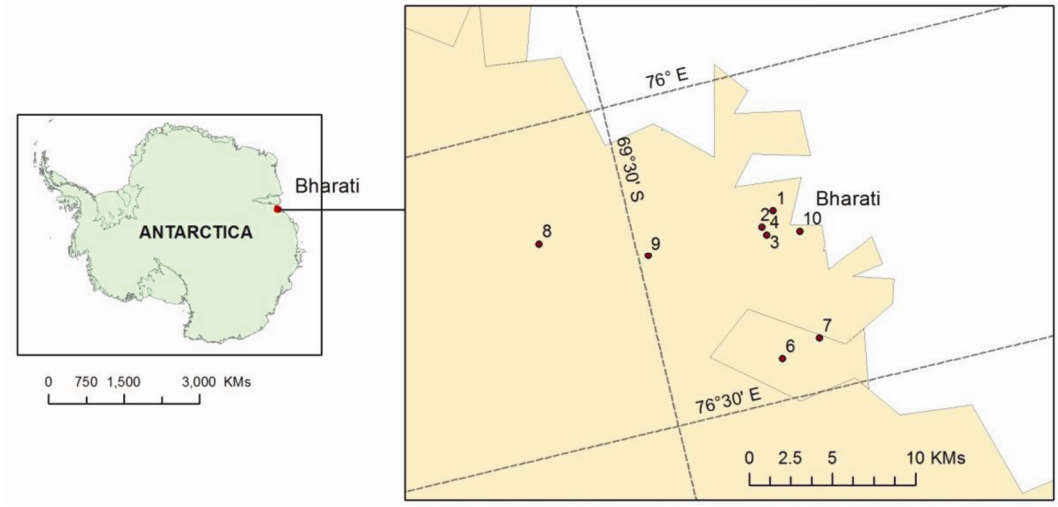

Figure 2. Index map showing location of observation points near Bharati station, Antarctica.

Field observations were carried out during the 35th Indian Scientific Expedition to Antarctica (ISEA) (austral summer of 2015–16) at Larsemann Hills, Antarctica to understand the relationship between melt/freeze conditions derived from scatterometer and field observations. The results of concurrent field observations on snowpack properties and their linkage with satellite-based observations are presented here.

Instruments used

The present study uses Geoscanners AB, Akula 9000 ground penetrating radar (GPR) from Sweden at 200 MHz frequency along with snow fork from Toikka Oy, Finland for measurement of snow density and liquid water content in the snow[12,13] (Figure 1). It is a microwave fork operating at frequency ~1 GHz, which measures the relative dielectric constant of snow. Both real and imaginary parts of the dielectric constant help in calculating density and wetness of snowpack, which are derived using empirical relations[14]. The average permittivity obtained using the snow fork represents a snow sample collected over effective length of ~6 cm and diameter ~2 cm (refs 13, 15, 16). Measurement range of snow density was 0–0.6 g/cm^3 and that of liquid water content from 0% to 10%.

Data and methodology

Field observations

Figure 2 and Table 1 provide details of observation points at Larsemann Hills near Bharati (60°15′S, 76°25′E) along with dates of observation. Hand-held Garmin Global Positioning System (GPS) was used to locate the points.

The snow fork observations were collected over the ice sheet by digging snow pit above the existing ice. The pits was dug carefully and as far as possible, the wall where observations were taken was not disturbed (Figure 3 *a*). In the shallow snow depth zone, the pit was dug till the hard ice was reached. Observations were taken immediately after digging to avoid melt by sun. Figure 3 *b* shows the sampling design for observations. It took about 2 min to complete one set of vertical observations. The fork tong was wiped before each observation. Visual observations were made at each pit for apparent characteristics, viz. hard crust, water flow, icy layers, etc. The snow pits showed different stratigraphic layers over ice sheet, indicating layered deposition of snow (Figure 3 *c*) along with hard refrozen snow firn in the observation pits. No flowing water was observed in the pits.

The snow fork was calibrated in the air before observations. The observed mean resonant frequency in air was

Table 1. Details of observation points

Point ID	Date	Observation time	Latitude	Longitude	Distance from coast (km)	Observation of	
1	15 December 2015	Forenoon	–69.4243	76.21475	1.4	GPR	Fork
2	15 December 2015	Forenoon	–69.4323	76.23494	2.48	GPR	Fork
3	26 December 2015	Evening	–69.4307	76.24825	2.58	GPR	Fork
4	31 December 2015	Forenoon	–69.4307	76.24828	2.57	GPR	Fork
6	5 January 2016	Forenoon	–69.4382	76.43831	5.19	GPR	
7	5 January 2016	Forenoon	–69.4163	76.42069	2.7	GPR	
8	5 January 2016	Afternoon	–69.5504	76.1785	15.53	GPR	Fork
9	6 January 2016	Forenoon	–69.4952	76.23681	9.3	GPR	Fork
10	6 January 2016	Forenoon	–69.4131	76.25481	0.50	GPR	

GPR, Ground penetrating radar.

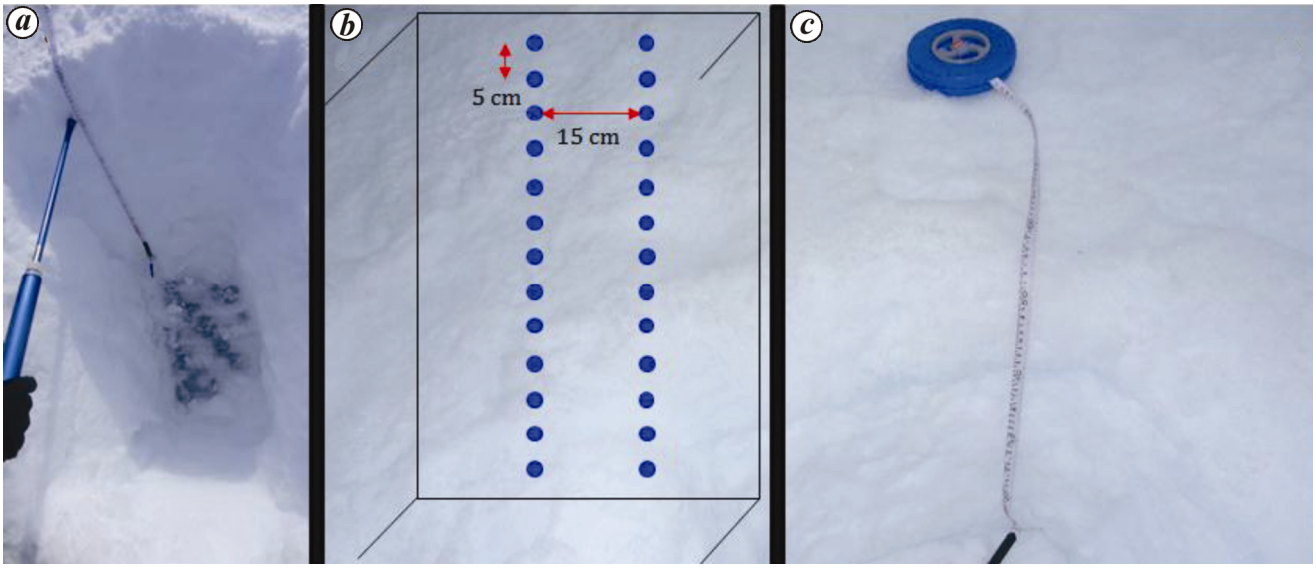

Figure 3. ***a***, Observation pit above ice crust; ***b***, Observation scheme; ***c***, Observation pit with snow firn layer.

892.7 ± 1.7 MHz, which is within measurable limits of the instrument. Since the snow fork had already been tested for its accuracy in calculating density and wetness, no further field samples were collected. Density and wetness observations were repeated several times on each side of snow pit and average observations were tabulated.

Satellite data

Advance Scatterometer (ASCAT) is an active microwave scatterometer mounted on satellites MetOp-A and MetOp-B, which acquires data in C-band at 5.26 GHz (5.7 cm wavelength) in vertical polarization (VV). This study utilized enhanced resolution daily products available at 4.45 km in Scientific Information Retrieval (SIR) format for the period 2011–2016. All pass products, where $\sigma°$ was normalized to 40° incidence angle were used in the study. Apart from ASCAT data, Oceansat-2 Scatterometer (OSCAT) data on-board Oceansat-2 in Ku band (13.6 GHz and HH polarization, 2.225 km) were also used for the period 2011–2014.

Temperature data

Automatic weather station (AWS) temperature data recorded by the Indian Institute of Geomagnetism (IIG), Navi Mumbai at Bharati station were used utilized in the study. Figure 4 shows the temperature profile during austral summer months (2015–16) along with the diurnal variation in temperature during observation days.

Results and discussion

Snow density and wetness measurements

Figure 5 shows the density and wetness profiles observed over six points (Table 1) with two observations at each point/pit. Since majority of measurements in 2015–16

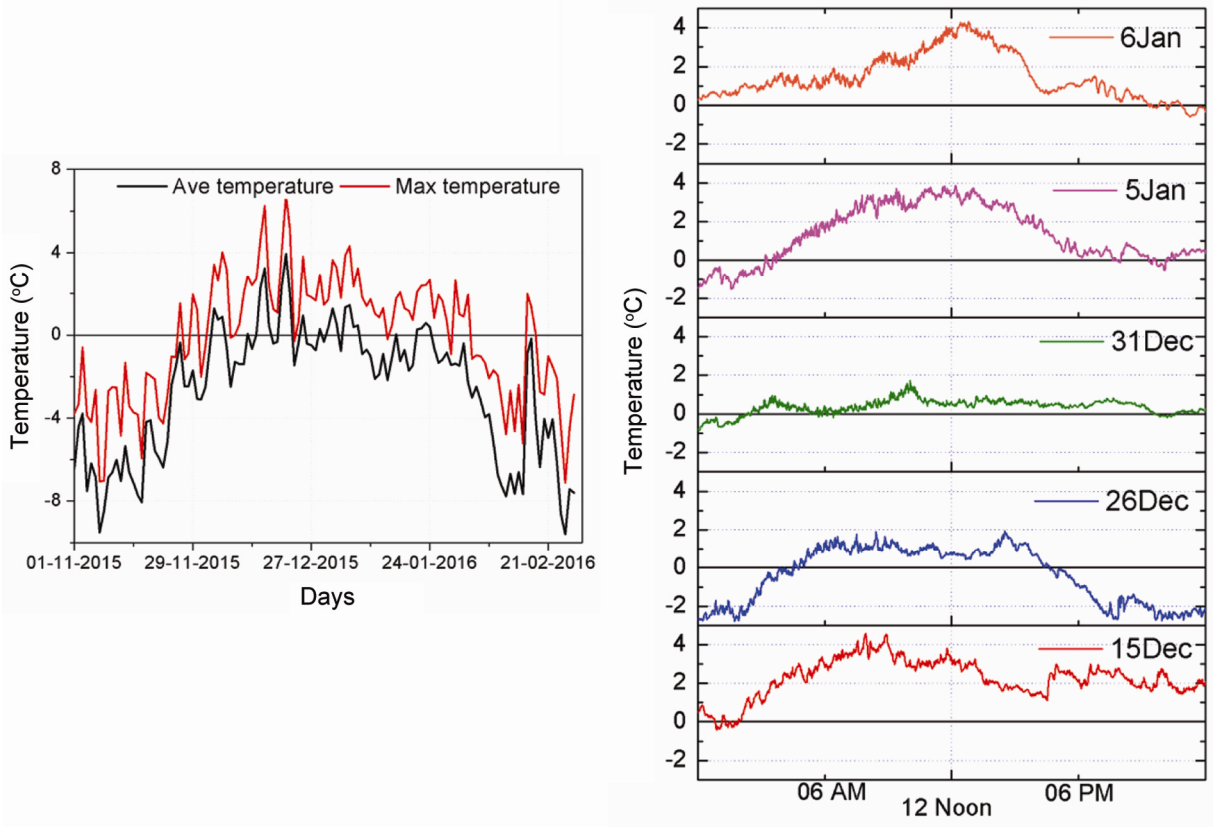

Figure 4. Austral summer temperature measured at Bharati station.

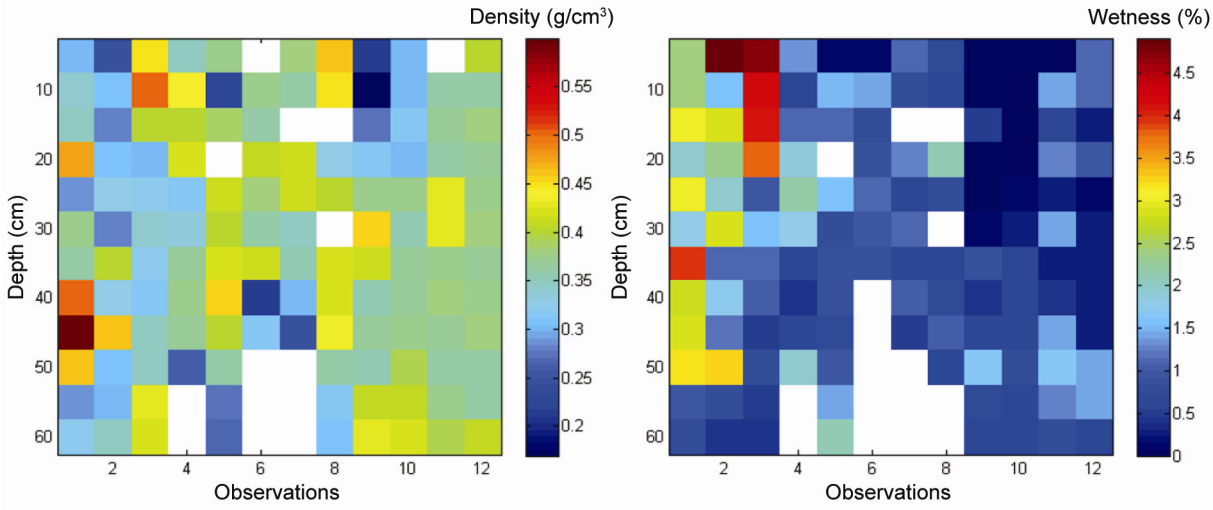

Figure 5. Vertical distribution of snow density and wetness over 12 observations near Bharati station. Measurements were taken at 5 cm vertical interval.

were up to 70 cm depth of snow, a comparison was made up to this depth only. The density varied between 0.17 and 0.6 g/cm^3. It was found to be affected by the presence of subsurface ice lenses or firn, which produced pronounced density contrast. The ice firn, which is formed when subsequent freezing of generated melt water takes place, is buried under annual accumulation layers. A decrease in density was observed just below the firn, which increased again with depth till another firn was encountered.

The water content measured at these locations varied between 0% and 4.9% by volume, which is well within the measuring limit of snow fork. Apart from one or two locations at the surface and near surface, majority of snow pack was observed in moist condition where water is not visible and when lightly crushed, the snow has a

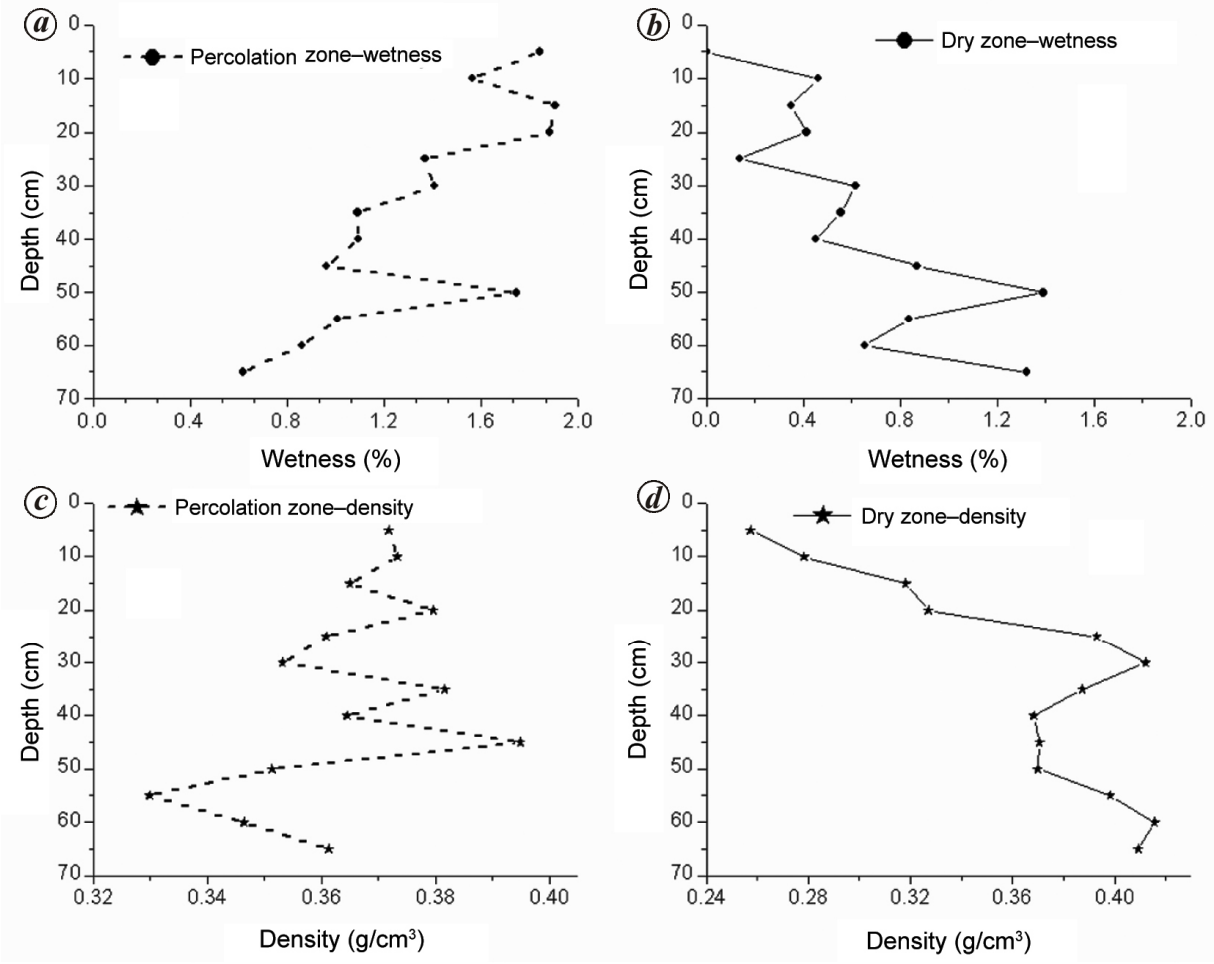

Figure 6 *a–d*. Average density and wetness on dry and percolation zones near Bharti station.

Table 2. Melt onset, freeze onset and melt days at observation points near Bharati station, Antarctica using ASCAT data

Event	2011–12	2012–13	2013–14	2014–15	2015–16*
Point 4					
Melt onset	21 December	11 December	29 December	18 December	14 December
Freeze onset	8 January	29 January	2 February	14 February	11 January
No. of melt days	13	50	37	27	17
Point 8					
Melt onset	No melt	3 January	1 January	No melt	19 December
Freeze onset	Freeze only	24 January	25 January	Freeze only	23 December
No. of melt days	Nil	28	24	6	4
Point 9					
Melt onset	No melt	17 December	1 January	22 December	17 December
Freeze onset	Freeze only	25 January	27 January	11 January	23 December
No. of melt days	2	40	26	15	6
Point 10					
Melt onset	27 December	9 December	30 December	18 December	14 December
Freeze onset	8 January	2 February	25 February	13 January	25 January
No. of melt days	16	53	30	29	19

*ASCAT data not available during 1–6 January and 14–20 January 2016.

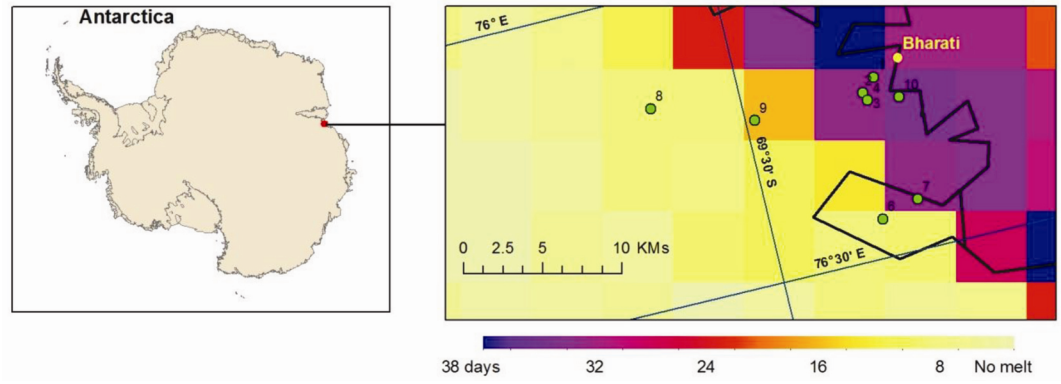

Figure 7. Number of melt days using ASCAT data near Bharati station.

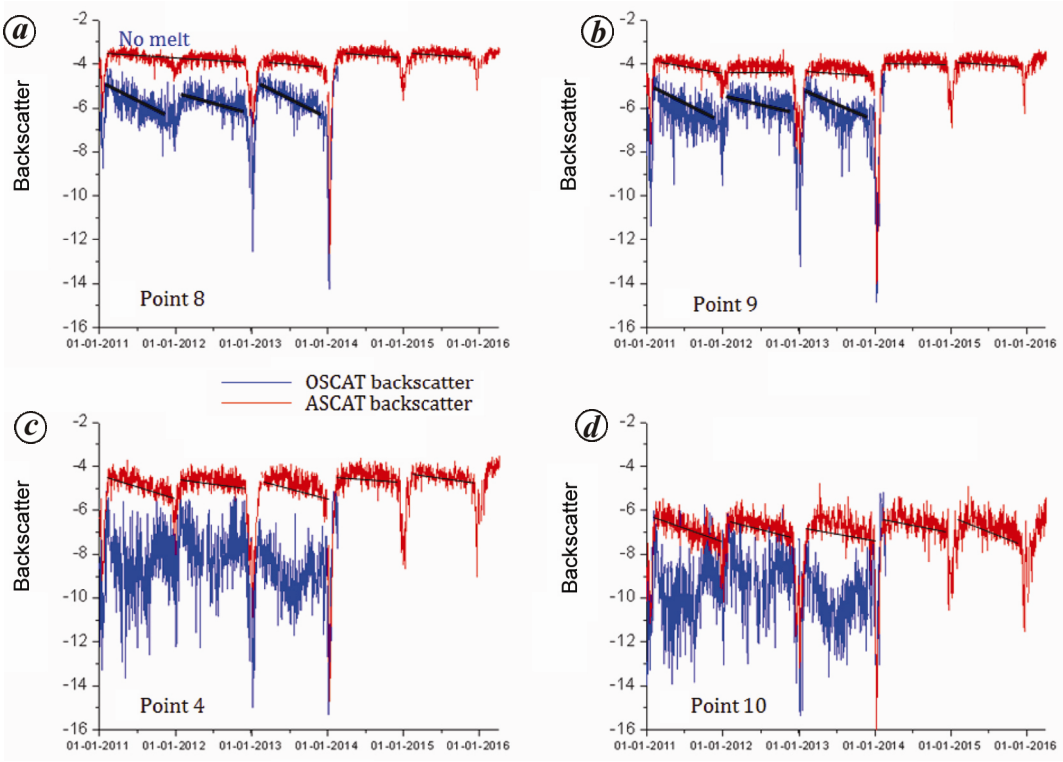

Figure 8 *a–d*. Snow accumulation and melt signatures over observation points with ASCAT (5.3 GHz) and OSCAT (13.6 GHz).

tendency to stick together[17]. In Figure 6, the average density and wetness are plotted separately as a function of depth for percolation and dry zones. Percolation zones are those areas where some surface melting may occur, but the melt water refreezes at a shallow depth. The observed data show a contrasting behaviour of wetness and density in both the zones. The wetness in the percolation zone shows a decreasing trend with depth (Figure 6 *a*), whereas a reverse trend is seen in the dry zone. The presence of subsurface firn and lenses has an effect on the wetness distribution as evident in Figure 6 *a*, with observed increase in wetness below the firn. The observations show the presence of major ice firn at around 50–55 cm depth even in the dry zone (Figure 6 *b*). The density curve shows an increasing trend with depth as expected for the dry zone (Figure 6 *d*), which is also affected by the presence of firn. More such layers have been recorded in the percolation zone during field observations, which can be clearly seen in the depth–density graph (Figure 6 *c*).

The observations made by Techel and Pielmeier[7] indicate a decrease in water content during the day in the snow profile at a few locations. Unless multiple observations are taken in a day at the same location, it is difficult to observe the diurnal change in water content. More attempts will be made in the 36th ISEA to collect field observations twice a day in order to know the changing pattern of diurnal wetness and density.

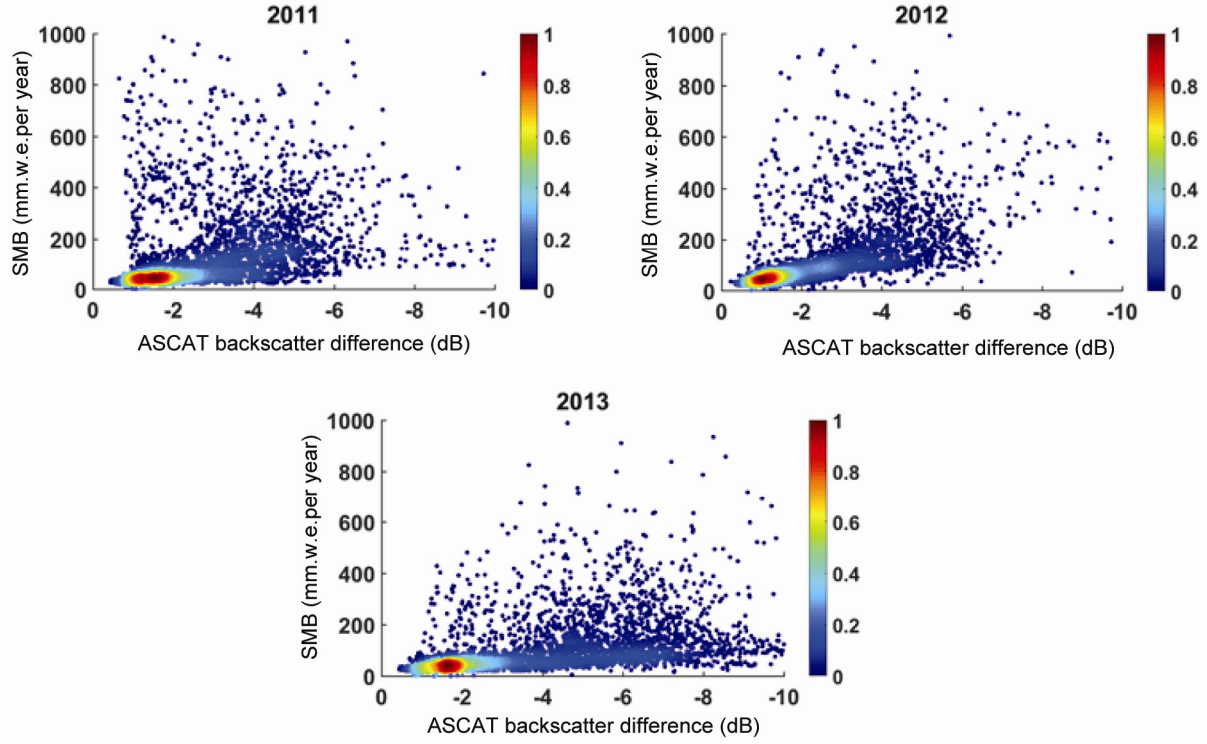

Figure 9. Surface mass balance accumulation (millimetre water equivalent) versus microwave backscatter-derived backscatter difference.

Melt/freeze analysis

Melt/freeze status analysis was carried out with ASCAT data for the period 2011–16 using the variable threshold methodology[10], where stable freezing season backscatter mean and standard deviation are used to identify the melt/freeze status at each location. Onset of melt is recorded when there is melt condition for continuous two days. Table 2 provides details about onset of melt, onset of freeze and number of melt days. Figure 7 shows a map of melt days for the year 2015–16. Lowest melting was mapped in the year 2011–12, which matches with the results of melt/freeze studies carried out using OSCAT and QuikSCAT data[10].

Melt and freeze onset days show spatiao-tempotal variability over observation points, with 2015–16 showing melt conditions at points 8, 9, 4 and 10 for 4, 6, 17 and 19 days respectively. Since the satellite data were not available for the period between 1 and 6 January as well as 14 and 20 January few crucial melt days could not be mapped.

The melt map was correlated with temperature observations near Bharati station, since no other observations were available on ice sheet. Five observations points were within 3 km, whereas the farthest point 8 was at 15.5 km from the coast. First positive temperature was recorded on 26 November 2015 (Figure 4), but the average temperature reached above melting point on 4 December and the temperature dropped again. The onset of melting occurred on 14 December (ASCAT), which coincided with the positive degree day (PDD). Melt days (MD) and PDD coincided for the year 2013–14. Similar observations were also made for the points 4 and 10 for other years. The correlation of MD vs PDD reduced with distance from the coast as the temperature in Antarctica varies drastically, even over short distances and the recorded temperature may not always be representative of the conditions even 1 km apart. Points 8 and 9 fall in the boundary between the percolation and dry snow zones, and the remaining points fall under the percolation zone. The snow profile observations of density at both snow zones confirmed the characteristics of the zones (Figure 6). Long-term analysis of variations in the areal extent of these zones will help in understanding the radiation budget, stability of ice sheet and ultimately the impact of/on climate change.

Backscatter response of satellite data towards snow accumulation and wetness

Available backscatter (σ^0) was plotted against time for ASCAT (VV) for the years 2011–2016 and OSCAT (HH) data till February 2014 (Figure 8). Active microwave remote sensing is sensitive to melt/freeze status and accumulation rates. Although the relationship between accumulation rate and backscatter is complex, comparative observation analysis was done here. Accumulation layer of snow over a scattering layer results in a decrease

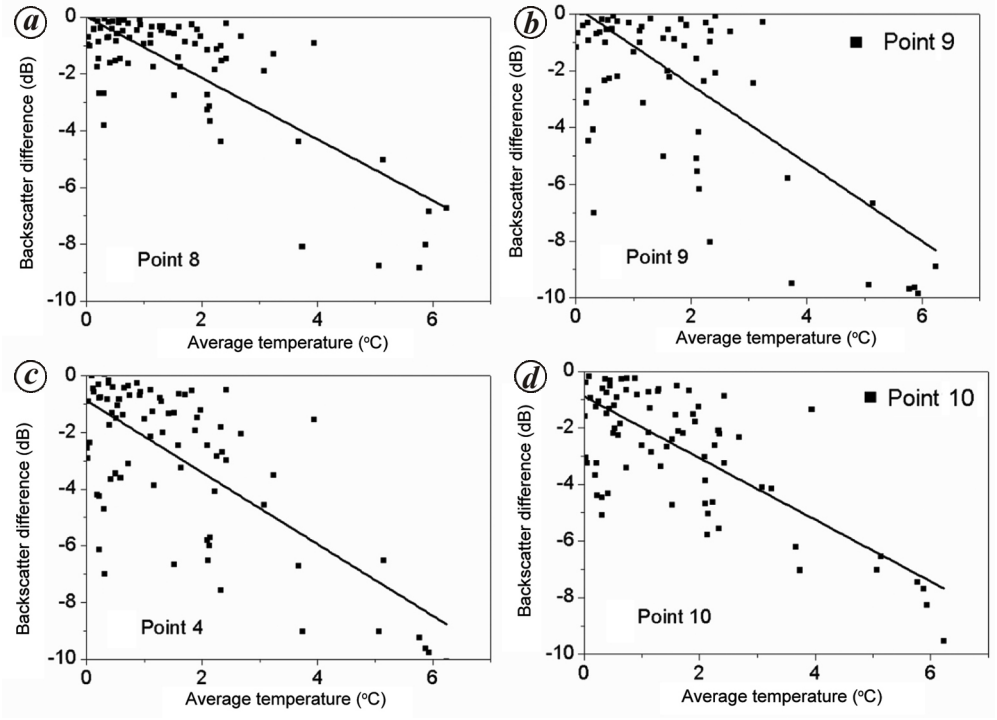

Figure 10 *a–d*. Scatter plot between difference of melt backscatter and winter backscatter, and average temperature.

in backscatter over time due to melt metamorphic of snow and firn layers[18]. Metamorphism is the change in snow crystal form due to heat flow and pressure. Associated changes are observed in the snowpack characteristics, viz. density, porosity, water content, strength, etc. due to this process. The observation points show an inverse relation between rate of accumulation and backscatter. Time series of points 8 (Figure 8 *a*) and 9 (Figure 8 *b*) under dry snow zone is different than points under accumulation zone. High backscatter in the dry snow zone is due to low accumulation rates, as the large grain size developed during low accumulation rates is responsible for high backscatter. The number of layers is related to the annual snowfall accumulation over the ice sheet. A negligible slope of ASCAT backscatter (red line) can be seen in the dry zone. In contrast to the graphs pertaining to the dry zone, the backscatter from the points 4 (Figure 8 *c*) and 10 (Figure 8 *d*) within the percolation zone shows varying accumulation rates over the years. At location 4 (Figure 8 *c*), a small backscatter decrease is observed during the years 2012 and 2014, indicating low snow accumulation rate and high density layer, whereas at location 10, high snow accumulation rate and a low density dominant layer result in relatively high backscatter decrease for the years 2011, 2013, 2015 (Figure 8 *d*). In comparison to ASCAT, OSCAT is more sensitive to volume scattering from fresh snow accumulation owing to smaller wavelength which allows for more interaction with the snow grain.

One of the marked differences in the behaviour of ASCAT and OSCAT backscatter is observed over the accumulation zone (Figure 8 *c* and *d*). The OSCAT backscatter shows reducing trend in the freezing winter and then an increase in backscatter is observed. Since the Ku band is sensitive to fresh snow accumulation, a change in backscatter pattern could be attributed to removal of accumulated layer by wind and other process. Another reason could be the formation of surface hoar layer, which increases backscatter values. C band was found to be more sensitive to accumulation rate change than the Ku band[19]. Since satellite data were not available for the field observation years, ground verification of the phenomena could not be carried out. With the availability of SCATSAT (launched in September 2016) data in the future expeditions, detailed field data acquisition is being planned.

Surface mass balance yearly map of RACMO2.3 version 2.3 (ref. 20) was used for correlating the backscatter response to snow accumulation and annual comparison was made between RACMO2.3 SMB and the freezing season σ^0 decrease, which is derived for each pixel for each year as the difference in backscatter at the start of freeze (σ^0_{Freeze}) and melt (σ^0_{Melt}).

$$\Delta\sigma^0 = \sigma^0_{\text{Freeze}} - \sigma^0_{\text{Melt}}. \quad (1)$$

Figure 9 shows the colour density scatter plot between ASCAT $\Delta\sigma^0$ and SMB for the years 2011, 2012 and 2013 for East Antarctica. Observations for the year 2013 indicate greater value of $\Delta\sigma^0$ in comparison to the years 2011 and 2012. A clear-cut relation did not emerge between these two variables, but it needs more observations and analysis.

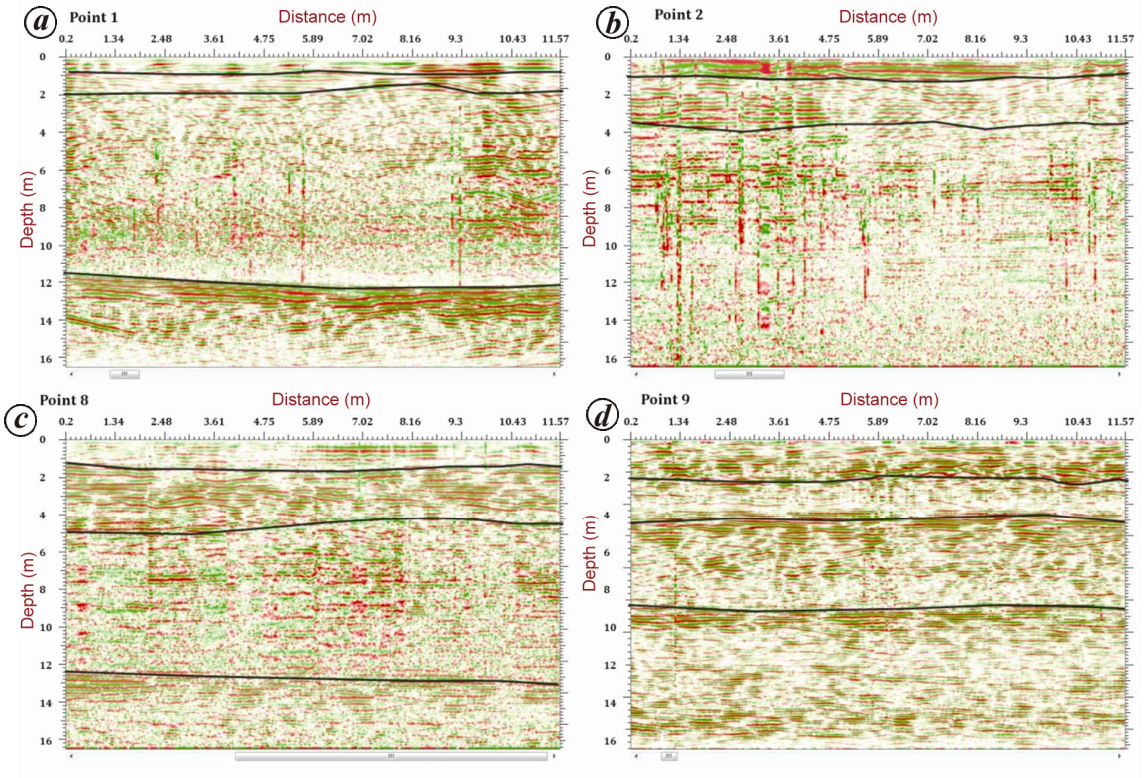

Figure 11 ***a–d.*** GPR profile over observation points 1, 2, 8 and 9.

Table 3. Correlation between difference of melt backscatter and winter backscatter and average temperature

Average temperature	Difference backscatter			
Observation points	Point 4	Point 8	Point 9	Point 10
Correlation	–0.70	–0.78	–0.69	–0.73

Melting snow causes a drop in the backscatter as surface scattering becomes dominant over volumetric scattering, thereby reducing the measured backscatter[21,22] (Figure 8). A correlation was found between the decrease in backscatter and PDD temperature over observation points (Figure 10). Figure 10 indicates the sensitivity of ASCAT backscatter to melt. Backscatter difference during melt was calculated for each year after finding the stable mean during austral winter. The slope of the regression line indicates that melt at points 8 and 9 (Figure 10 *a* and *b* respectively) in the dry zone is not initiated immediately at PDD. The slope of regression line at points 4 and 10 (percolation zone) indicates the sensitivity of the microwave sensor to detect subsurface backscattered or emitted radiation, and accordingly, even when the surface is frozen with temperature below zero, some melt is detected, which might have occurred due to radiative forcing.

Table 3 shows the correlation between backscatter difference and temperature for observation points with maximum correlation observed at point 8. Since the number of observations is less, no correlation could be found. The same will be attempted in the 36th Antarctic expedition.

GPR profiles at observation points

Figure 11 shows sample GPR profiles over four observation points. Radar profiles were subjected to post-processing techniques to make them more readable and understandable. Time zero correction was applied after identifying the first positive peak in the returning signal. Background removal step removed the effect of directed wave. The use of high-pass filter helped in determining the valid and background signals. Gain correction was done to highlight areas of particular interest or importance. A reflecting layer due to change in dielectric constant at around 0.8 m coincides well with field pit observations of snow over hard ice at locations 1 and 2 (Figure 11 *a* and *b*). Rocky bottom at 11.5 m is visible in the profile at point 1. With 200 MHz radar antenna, penetration depth of 17 m was obtained. Presence of different reflecting layers can be seen in the GPR profile, which needs further correlation with snow accumulation rates at points 8 and 9.

Conclusion

Analysis of field observations collected using snow fork and GPR at Larsemann Hills, East Antarctica during the 35th ISEA in austral summer of 2015–16 is reported here. Average density and wetness for the dry and percolation

zones showed contrasting behaviour for observed locations. Analysis of ASCAT and OSCAT was carried out to understand melt/freeze status. Identified dry and percolation zones matched with the field observations of density and wetness. Observed density reduced at ice firn in the snow pack. The number of melt days varied spatially and temporarily, with the year 2011–12 being the coldest in last five years. The analysis results correlated well with PDD. There was large variability in temperature on the observation days with day temperature varying between 1°C and 4°C, which was correlated with change in backscatter response. Backscatter response of ASCAT and OSCAT varied for snow accumulation, which needs further validation using more field observations. The response of scatterometer to change in liquid water content by melting snow showed a correlation of 0.78 with PDD and also with a few field observations. ASCAT observations showed low correlation with surface mass balance, but further detailed analysis is needed for the dry and percolation zones separately. The field database serves as baseline data for validation of the recently launched satellite SCATSAT from India. Further detailed observations to cover diurnal variations in snowpack conditions are being planned during the 36th ISEA in 2016–17.

1. Tedesco, M., Remote sensing of the cryosphere. In *Library of Congress Cataloging-in-Publication Data* (ed. Tedesco, M.), Wiley Blackwell, 2015.
2. Gupta, R. P., Haritashya, U. K. and Singh, P., Mapping dry/wet snow cover in the Indian Himalayas using IRS multispectral imagery. *Remote Sens. Environ.,* 2005, **97**(4), 458–469.
3. Singh, K. K., Kumar, A., Kulkarni, A. V., Datt, P., Dewali, S. K. and Kumar, M., Experimental investigation of dielectric properties of seasonal snow at field observatories in the northwest Himalaya. *Ann. Glaciol.*, 2016, **57**(71), 319–327.
4. Shiraiwa, T. H., Saito, T., Yokoyama, K. and Watanabe, O., Structure and dielectric properties of surface snow along the traverse route from coast to Dorne Fuji station, Queen Maud land, Antarctica. In Proceedings of National Institute of Polar Research Symposium. *Polar Meteorolo. Glaciol.*, 1996, **10**, 1–12.
5. Karkas, E., Martma, T. and Sonninen, E., Physical properties and stratigraphy of surface snow in Western Dronning Maud land, Antarctica. *Polar Res.*, 2005, **24**(1–2), 55–67.
6. Sugiyama, S., Enomoto, H., Fujita, S., Fukui, K., Nakazawa, F. and Holmlund, P, Dielectric permittivity of snow measured along the route traversed in the Japanese–Swedish Antarctic Expedition 2007/08. *Ann. Glaciol.*, 2010, **51**(55), 9–15.
7. Techel, F. and Pielmeier, C., Point observations of liquid water content in wet snow – investigating methodical, spatial and temporal aspects. *Cryosphere*, 2011, **5**, 405–418.
8. Zwally, H. J. and Fiegles, S., Extent and duration of Antarctic surface melting. *J. Glaciol.*, 1994, **40**, 463–476.
9. Liu, H., Wang, L. and Jezek, K. C., Automated delineation of dry and melt snow zones in Antarctica using active and passive microwave observations from space. *IEEE Trans. Geosci. Remote Sensing*, 2006, **44**(8), 2152–2163.
10. Bothale, Rajashree V., Rao,P. V. N., Dutt, C. B. S., Dadhwal, V. K. and Maurya, D., Spatio-temporal dynamics of surface melting over Antarctica using OSCAT and Quik SCAT scatterometer data (2001–2014). *Curr. Sci.*, 2015, **109**(4), 733–744.
11. Oza, S. R., Spatial-temporal patterns of surface melting observed over Antarctic ice shelves using scatterometer data. *Antarct. Sci.*, 2015, 1–8.
12. Sihvola, A. and Tiuri, M., Snow fork for field determination of the density and wetness profiles of a snow pack. *IEEE Trans. Geosci. Remote Sensing*, 1986, **GE-24**, 5.
13. Snow fork: a portable instrument for measuring properties of snow (brochure), Toikka Engineering Ltd, Espoo, Finland, 2010; http://www.toikkaoy.com
14. Denoth, A., An electronic device for long-term snow wetness recording. *Ann. Glaciol.*, 1994, **19**, 104–106.
15. Tiuri, M. T., Sihvola, A. H., Nyfors, E. G. and Hallikainen, M. T., The complex dielectric constant of snow at microwave frequencies. *IEEE J. Ocean. Eng.*, 1984, **9**(5), 377–382.
16. Fierz, C. and Föhn, P., Long-term observation of the water content of an Alpine snowpack. In Proceedings of the International Snow Science Workshop, 30 October–3 November 1994, Snowbird, UT, 1994, pp. 117–131.
17. Fierz, C. R. L. A. *et al.*, The International Classification for Seasonal Snow on the Ground, IHP-VII Technical Documents in Hydrology N83, IACS Contribution N1, UNESCO-IHP, Paris, 2009.
18. Long, D. and Drinkwater, M., Greenland ice sheet surface properties observed by the Seasat – a scatterometer as enhanced resolution. *J. Glaciol.*, 1994, **40**(135), 213–230.
19. Dierking, W., Linow, S. and Rack, W., Toward a robust retrieval of snow accumulation over the Antarctic ice sheet using satellite radar. *J. Geophys. Res.*, 2012, **117**, DO9110.
20. Wessem, J. V. M. *et al.*, Improved representation of East Antarctic surface mass balance in a regional atmospheric climate model. *J. Glaciol.*, 2014, **60**, 761–770.
21. Ulaby, F. T., Moore, R. K. and Fung, A. K., *Microwave Remote Sensing: Active and Passive, Vol. I – Microwave Remote Sensing Fundamentals and Radiometry*, Addison-Wesley, Advanced Book Program, Reading, Massachusetts, USA, 1981, p. 456.
22. Tedesco, M., Kim, E. J., England, A. W., De Roo, R. D. and Hardy, J. P., Brightness temperatures of snow melting/refreezing cycles: observations and modeling using a multilayer dense medium theory-based model. *IEEE Trans. Geosci. Remote Sensing*, 2006, **44**(12), 3563–3573.

ACKNOWLEDGEMENTS. R.V.B. and S.A. thank the Indian Space Research Organization for permission to participate in the 35th ISEA, and the National Centre for Antarctic and Ocean Research, Ministry of Earth Sciences, Government of India for making all the necessary arrangements for this expedition. We thank IIG, Mumbai for providing the AWS data for Bharati station; Dr Ajay Dhar (IIG, Mumbai) for ground truth and other support received; Dr Shrivastava (GSI), Shri K. Venkat Raghvendra (Bharati station) and all members of 35th ISEA for providing support during expedition. R.V.B. and S.A. also thank Dr P. V. N. Rao (Earth and Climate Science Area (ECSA), NRSC) and Dr C. B. S. Dutt (ECSA) for encouragement and guidance in taking up this activity.

Received 13 October 2016; revised accepted 21 March 2017

doi: 10.18520/cs/v113/i04/733-742